ORIGINAL PAPER

Risk assessment of water inrush to coal seams from underlying aquifer by an innovative combination of the TFN-AHP and TOPSIS techniques

Longqing Shi [1,2] · Mei Qiu [1,2] · Chao Teng [3] · Ying Wang [2] · Tianhao Liu [2] · Xingyue Qu [2]

Abstract

Coal seam exploitation in many coal mines of North China coalfields is threatened by water hazards from underlying aquifers. Resolving the potential risk zonation of water inrush to prevent and control flood water disasters is important and challenging work. To effectively assess the risk of water inrush from the Ordovician aquifer to the exploitation of the No. 11 coal seam in the Zhaizhen coal mine, Xinwen coalfield, China, this paper proposes a water inrush risk index (WIRI) model based on a combination of the triangular fuzzy number (TFN), analytic hierarchy process (AHP), and Technique for Order Performance by Similarity to Ideal Solution (TOPSIS) methods. The WIRI model integrates seven factors, namely, the water abundance of the Ordovician limestone aquifer, water pressure of the Ordovician limestone aquifer, aquifuge thickness, brittle rock percentage within the aquifuge, fault intensity index, fault endpoint and intersection density, and height of the mine-damaged zone, and was established using the TOPSIS method based on the initial decision data and the factor weights determined by the TFN-AHP method. The potential water inrush risk zonation was finally determined by the WIRI method. There are two zones in the study area: the safe area, and the dangerous area which was further classified into two subzones including the moderately dangerous area and the extremely dangerous area, providing guidance for engineers to predict and control floor water inrush. The predictions were validated by limited water inrush cases and safe mining samples. The results predicted by the WIRI method conform to the actual results, while the predictions by the T method do not agree well with the observation: with the T method, the three water inrush samples were judged to be safe. These results indicate that the proposed method can effectively predict water inrush risk and can be extended to other mines threatened by an underlying aquifer.

Keywords Coal mine · Water inrush · Risk assessment · TFN-AHP method · TOPSIS method · China

Introduction

The coal seams of the North China coalfields deposited in the Permo-Carboniferous period are typically exploited via underground mining. Mining is a high-risk technique, and mine accidents, such as gas and coal dust explosions and water inrush accidents, of which water inrush accidents cause major financial loss and are challenging to recover from in terms of production (Zhao et al. 2018; Zhang et al. 2017), occur frequently (Shi et al. 2019a; Wang and Meng 2018; Yang et al. 2019). The coal seams of the Shanxi Formation in the North China coalfields have been nearly fully exploited, and the deeply buried coal seams in the Taiyuan Formation constitute the main working bed. With the deepening of mines, their hydrogeological conditions are becoming increasingly complicated (Tan et al. 2010; Wu et al. 2017a). The exploitation of the deeply buried coal seams in the Taiyuan Formation is seriously threatened by floor water inrush, especially in the Ordovician limestone aquifer (Sun et al. 2015; Yin et al. 2015). According to statistics, over 200 water inrushes from the Ordovician aquifer have occurred in the past forty years, causing an estimated 30 billion yuan in losses and killing

✉ Mei Qiu
skdqiumei@126.com

1 Shandong Provincial Key Laboratory of Depositional Mineralization & Sedimentary Minerals, Qingdao 266590, China

2 College of Earth Sciences & Engineering, Shandong University of Science and Technology, Qingdao 266590, China

3 Qingdao Ruiyuan Engineering Group Co., Ltd., Qingdao 266555, China

approximately 1300 people (Shi et al. 2019a). Therefore, assessing the risk of floor water inrush is essential for helping control floor water hazards.

Numerous methods have been developed to assess floor water inrush risk over the past several decades. The water inrush coefficient method, T method, proposed in 1964 is widely used for predicting water inrush risk in China; this approach defines a specific value between aquifer water pressure and aquifuge thickness (Wu et al. 2011), involving only two controlling factors. However, water inrush involves many factors: water pressure, aquifuge thickness and water-resisting strength, water abundance, fractures, and mining disturbance. With the development of artificial intelligence, many methods have been widely used in various aspects of engineering (Hashemi et al. 2019; Norouzi and Namin 2019; Qu et al. 2019; Qiu et al. 2017; Bednarik 2019; Wu and Zhou 2008). The analytic hierarchy process (AHP) (Wu and Zhou 2008), artificial neural network (ANN) (Wu et al. 2008), fuzzy mathematics method (FMM) (Wang et al. 2012), support vector machine (SVM) (Shi et al. 2017), unascertained measure theory (UMT) (Wu et al. 2017b), random forest (RF) (Zhao et al. 2018), and entropy weight method (EWM) (Shi et al. 2019a) have been used for assessing water inrush to address the limited accuracy of the water inrush coefficient method and play an important role in the evaluation of water inrush risk by integrating multiple factors. However, these methods have certain limitations in practical applications. The AHP method has many potential advantages for assessing water inrush risk by integrating multiple factors, but the weights of the factors are determined based on expert opinions, with subjective judgments that vary for different individuals; ANN and RF methods are limited because of overlearning and local minima (Shi et al. 2019a); for the FMM, the division of the evaluation index grading lacks scientific evidence; the SVM model is limited due to its complex mathematical functions; for UMT, the constant weights of the factors are assigned by subjective expert opinions; and EWM requires a large number of water inrush sample data.

Accordingly, in this paper, a new model for risk assessment of water inrush from an underlying aquifer was proposed based on the combination of the triangular fuzzy number (TFN), AHP, and Technique for Order Performance by Similarity to Ideal Solution (TOPSIS) methods. TOPSIS method, a nonlinear method, is a commonly used and effective method in multi-attribute decision-making analysis, which can evaluate the relative risk of existing assessment samples according to their proximity to idealized targets (Hwang and Yoon 1981). For TOPSIS method, it is necessary to determine the weights of assessment factors. AHP-TFN method was applied to determine the weights of the assessment factors, which can deal with vagueness of human thought and uncertainty in real-world decision problems. And then the water inrush risk index (WIRI) model was

established by TOPSIS method based on the original values of factors and the weights calculated by AHP-TFN method, by which a zoning map of the water inrush risk of the No. 11 coal seam from the Ordovician aquifer in the Zhaizhen coal mine was developed for providing a scientific basis for safe production.

Study area

The Zhaizhen coal mine lies in the northern Xinwen coalfield, Shandong Province, China (Fig. 1), covering an area of approximately 13.58 km^2; the Zhaizhen coal mine is a North China coalfield.

From oldest to youngest, the stratigraphy in the Zhaizhen coal mine consists of the Ordovician system (S), Carboniferous S, Permian S, Paleogene S, and Quaternary S (Fig. 2). The coal-bearing strata in the Zhaizhen coal mine, which was deposited during the Permo-Carboniferous period, include six minable seams: from top to bottom, the Nos. 2 and 4 coal seams in the Shanxi Formation (F) and the No. 6 coal seam in the Taiyuan F, which have been exhausted, and the Nos. 11, 13, and 15 coal seams in the Taiyuan F, which are being exploited now. The aquifers below the No. 11 coal seam are: the sandstone fractured aquifer and thin limestone aquifers of the Taiyuan F and the Ordovician karst aquifer. The thin sandstone fractured aquifer and limestone aquifers of the Taiyuan F have poor water abundance and therefore do not pose a serious risk to the mining of the No. 11 coal seam. In contrast, with the characteristics of high hydraulic pressure, considerable thickness of more than 800 m and good water abundance and permeability, the Ordovician karst aquifer provides the primary risk to the exploitation of the No. 11 coal seam.

The formation that is targeted in the Xinwen coalfield, which is affected by tectonic movement, forms a monocline dipping NNE, with gentle dips less than 25°. Primarily striking NW, NEE, and NE, the faults are well developed. In particular, the No. 10 fault (F_{10} in Fig. 1) and its branch faults, striking NW, cut the Xinwen coalfield into a southern zone and a northern zone (Fig. 1). The southern zone includes the Xiezhuang and Huayuan coal mines and parts of the Liangzhuang, Suncun, and Huaheng coal mines. The northern zone includes the Zhaizhen coal mine and parts of the Liangzhuang, Suncun, and Huaheng coal mines. The No. 11 coal seam is buried shallowly and the Ordovician limestone aquifer has low water pressure in the southern zone, allowing safe mining of the No. 11 coal seam, while it is opposite for the northern zone. In part of the northern zone, the No. 11 coal seam was mined, but during this mining, three Ordovician karst water inrushes occurred in the Liangzhuang and Suncun coal mines. During these three inrush events, the maximum water yield reached 772.2 m^3/h, 78 m^3/h, and 50 m^3/h,
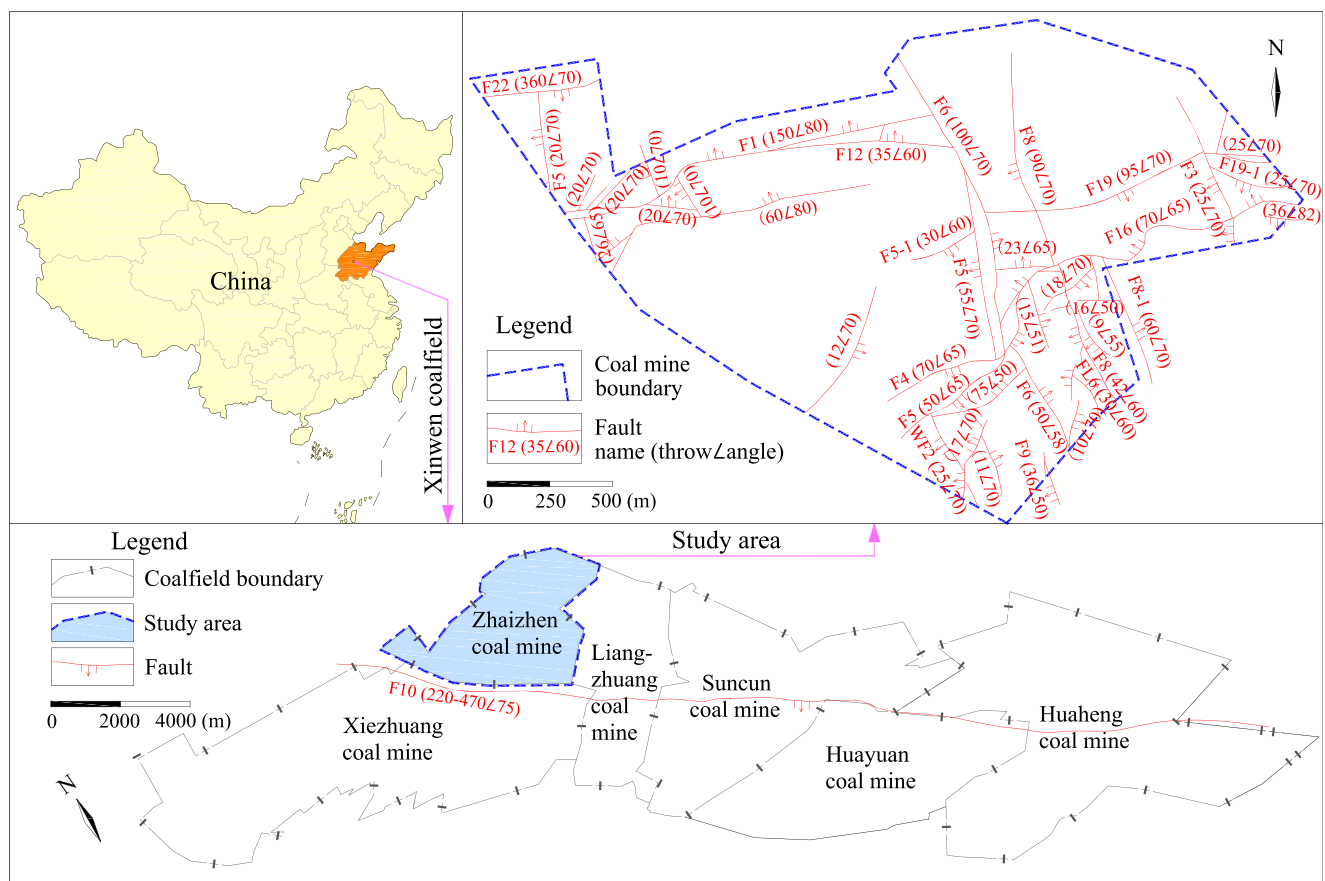
Fig. 1 Location of the study area in Shandong Province, China, and the geological structure of the Zhaizhen coal mine

respectively. Although parts of the No. 11 coal seam have been safely mined west of the Zhaizhen coal mine, the hydrogeological conditions are more complicated with increasing mining depth, which will make the mining of the No. 11 coal seam more dangerous.

Methodology

Procedures

Risk assessment of water inrush to coal seams from underlying aquifer based on the proposed combination method of the TFN-AHP and TOPSIS techniques includes four main steps (Fig. 3): (a) selecting the main assessment factors controlling floor water inrush and collecting geological data, (b) determining the weights of the assessment factors, (c) building WIRI model, and (d) validation, description of the results, and application.

Selecting factors controlling floor water inrush

According to engineering experience, many aspects affect water inrush, but there are four main aspects: aquifer, aquifuge,

geological structure, and mining. According to the systemic analysis of the major controlling factors (Wu et al. 2007; Wu and Zhou 2008), some relevant literature on this subject (Li and Chen 2016; Qiu et al. 2017; Shi et al. 2017, 2019a, b; Wu et al. 2011; Wu et al. 2015), and the hydrogeological conditions of the research area, these four aspects affecting water inrush and seven assessment factors were selected.
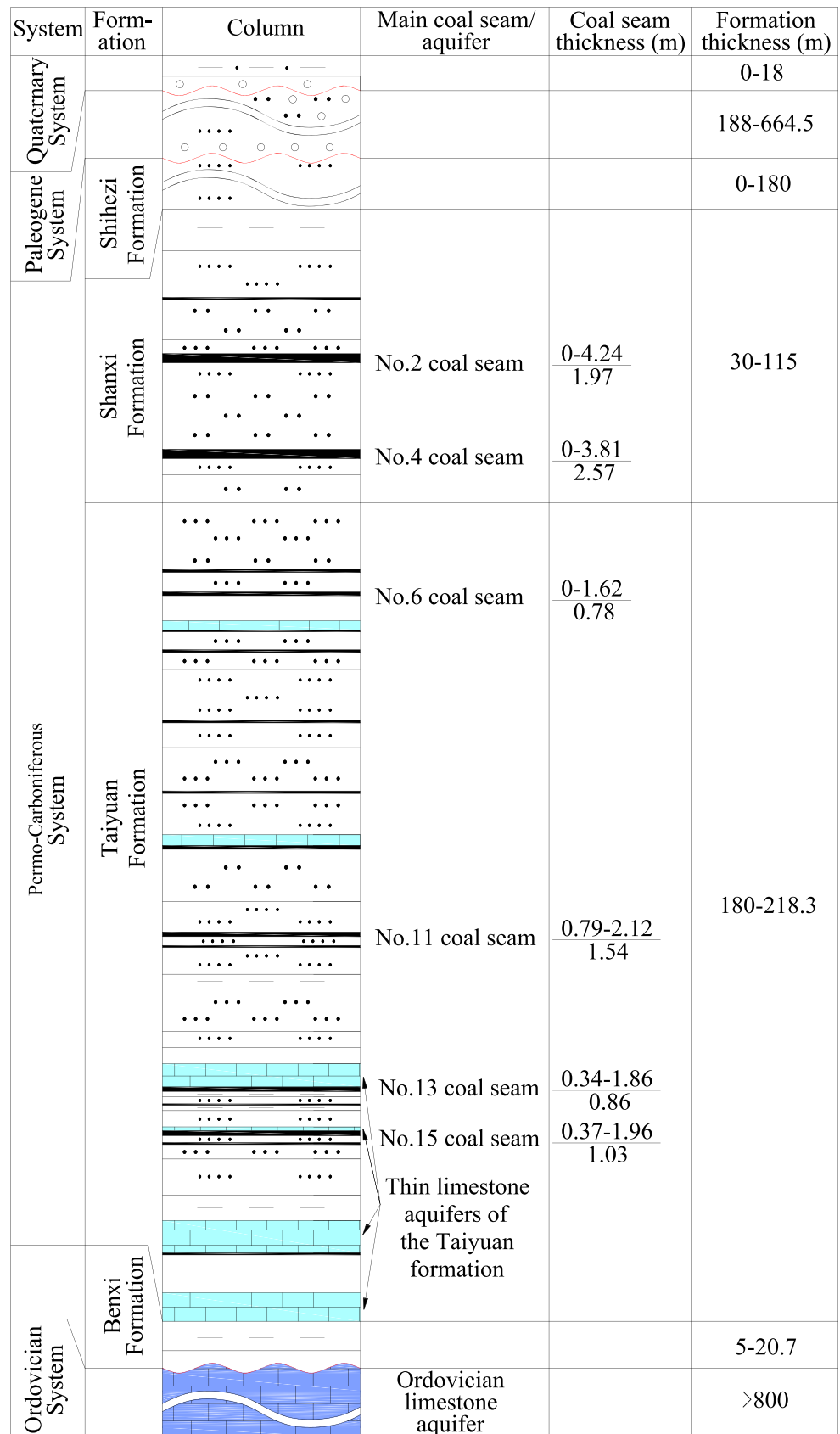
- *Aquifer* (F_1)

The properties of aquifers are important factors influencing floor water disasters (Li and Chen 2016). The properties of the Ordovician limestone aquifer are reflected via two components: the water abundance (F_{11}) and the water pressure (F_{12}).

- *Aquifuge* (F_2)

An aquifuge acts as a geologic barrier for preventing floor water inrush, and its water-resisting ability is closely related to its thickness and mechanical strength (Qiu et al. 2017). Therefore, the aquifuge index is as follows: aquifuge thickness is defined as the vertical distance from the No. 11 coal seam floor to the roof of the Ordovician limestone aquifer (F_{21}), and the brittle rock percentage

Fig. 2 Stratigraphic column of
the Zhaizhen coal mine

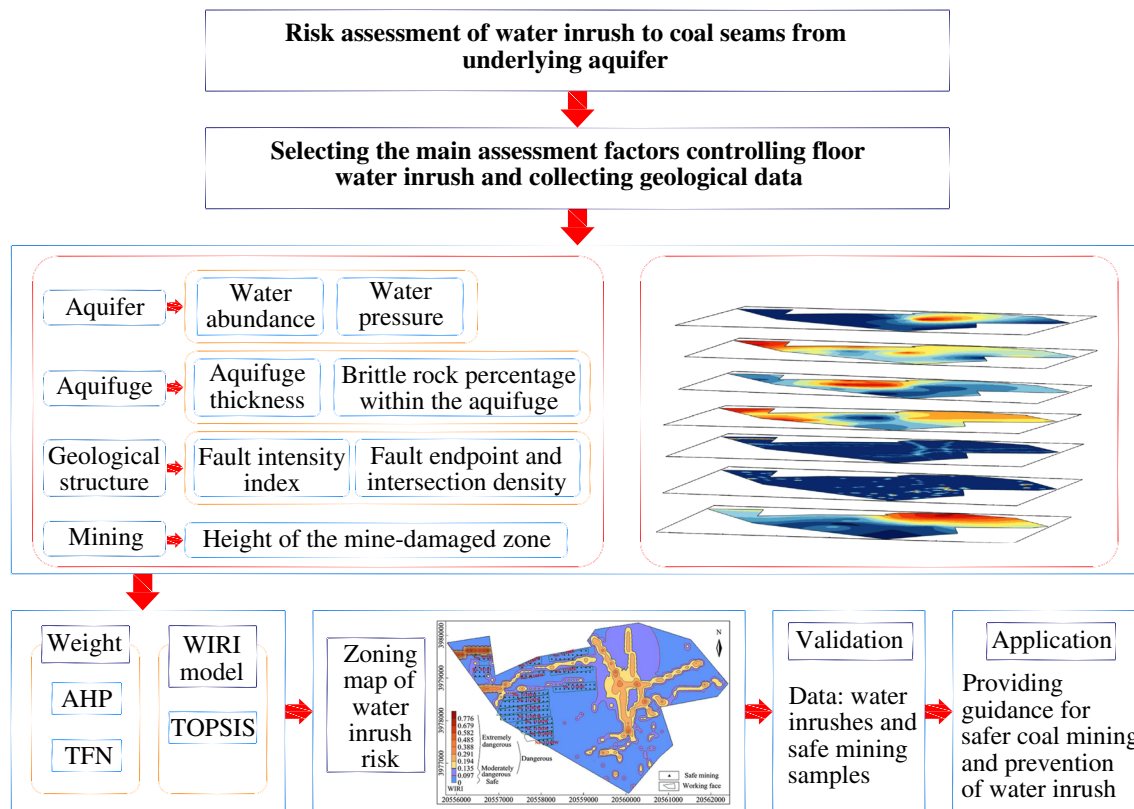| System	Form-ation	Column	Main coal seam/aquifer	Coal seam thickness (m)	Formation thickness (m)
Quaternary System					0-18
					188-664.5
Paleogene System	Shihezi Formation				0-180
Permo-Carboniferous System	Shanxi Formation		No.2 coal seam	$\frac{0\text{-}4.24}{1.97}$	30-115
			No.4 coal seam	$\frac{0\text{-}3.81}{2.57}$	
	Taiyuan Formation		No.6 coal seam	$\frac{0\text{-}1.62}{0.78}$	180-218.3
			No.11 coal seam	$\frac{0.79\text{-}2.12}{1.54}$	
			No.13 coal seam	$\frac{0.34\text{-}1.86}{0.86}$	
			No.15 coal seam	$\frac{0.37\text{-}1.96}{1.03}$	
			Thin limestone aquifers of the Taiyuan formation		
Ordovician System	Benxi Formation				5-20.7
			Ordovician limestone aquifer		>800

Fig. 3 Study flow in this paper

within the aquifuge reflects the mechanical strength of the aquifuge (F_{22}).

- *Geological structure* (F_3)

Geological structure has a strong influence on water inrush (Li 2000); the water inrush is dominated by the fault structure in the study area, which is determined by two properties: (1) the fault intensity index (F_{31}) defined as Eq. (1) (Shi et al. 2019a; Xu et al. 1991); and (2) the fault endpoint and intersection density (F_{32}).

$$F_{31} = \frac{\sum_{i=1}^{n} H_i \cdot L_i}{S} \qquad (1)$$

where F_{31} is the fault intensity index; H is the throw of the fault (m); L is the length of the fault in the strike direction (m); S is the area of the grid (m^2); and i, where $i = 1, 2, \ldots, n$, and n, is the number of faults in the grid.

- *Mining* (F_4)

The mine pressure that develops during mining activities will destroy the rock of a coal seam floor. The mine-damaged zone caused by the mine pressure is an important triggering factor of floor water inrush. The height of the mine-damaged zone (F_{41}) is selected and

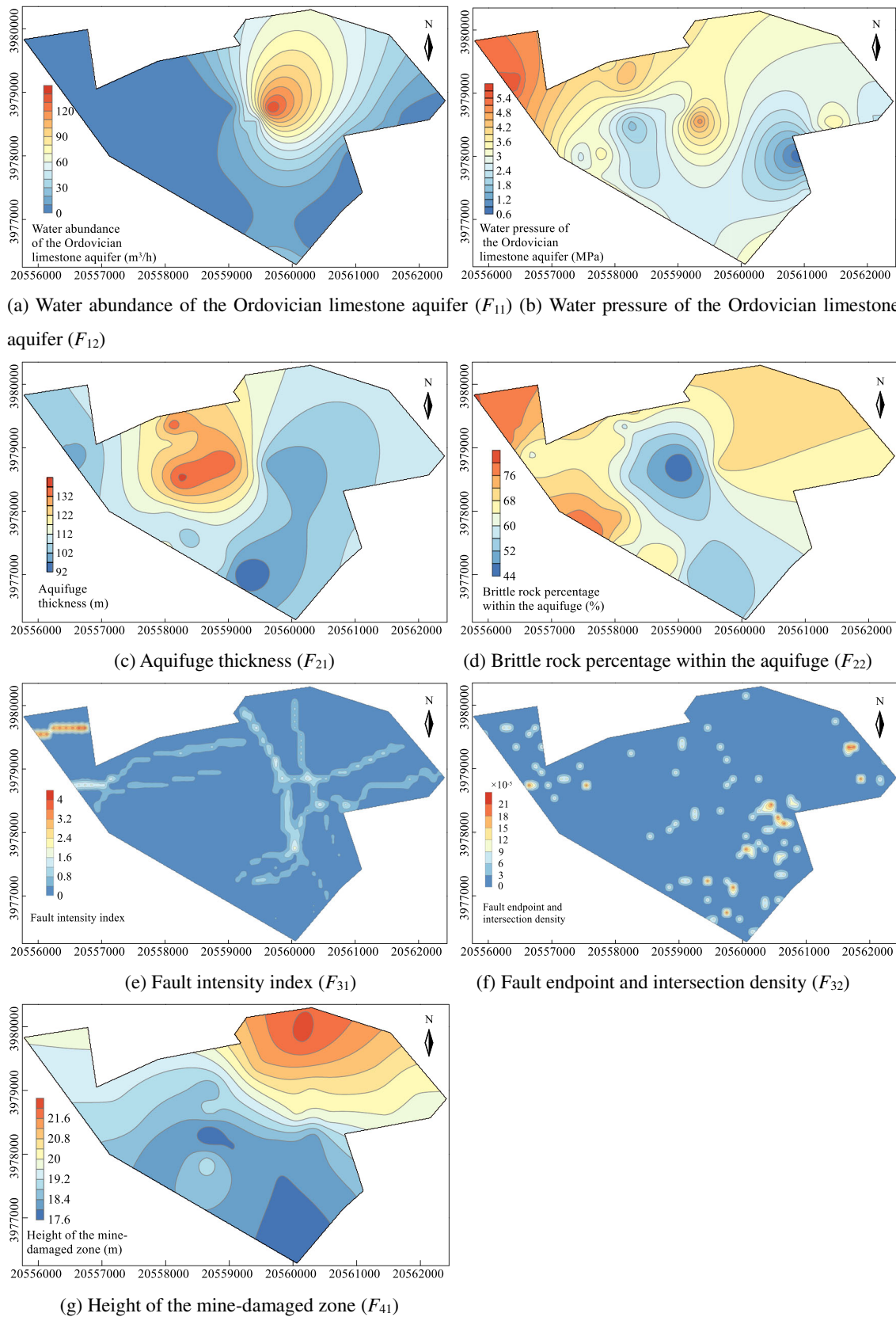computed by Eq. (2) (National Bureau of Coal Industry of China 2000):

$$F_{41} = 0.0085H + 0.1665\alpha + 0.1079L - 4.3579 \qquad (2)$$

where H is the depth of the mining (m); α is the coal seam dip angle (°); and L is the mining width of the mining face (m).

Seven main assessment factors were gathered, and then a contour map of each assessment factor in the study area was created using Golden Software Surfer 13.0, which has effective spatial analysis functions of space overlapping and drawing contour maps (Yin et al. 2018), as shown in Fig. 4.

Determining the weights of the assessment factors

Determining the weights of the assessment factors is critical for assessing the water inrush risk. Several methods have been developed to calculate the weights, such as the weighting factor, statistical index, and AHP methods. The AHP method, proposed first by T. L. Saaty (Saaty 1980), is very useful for multi-attribution decision-making problems (Chang et al. 2007; Wang et al. 2012). To set up the framework of the AHP analysis, it is essential to construct comparison matrices evaluated by the Delphi method (Tahriri et al. 2014), which collect exact values given by the decision maker about the relative importance of issues. However, the natural environment of the problems would make it hard for decision makers

(a) Water abundance of the Ordovician limestone aquifer (F_{11}) (b) Water pressure of the Ordovician limestone aquifer (F_{12})

(c) Aquifuge thickness (F_{21})

(d) Brittle rock percentage within the aquifuge (F_{22})

(e) Fault intensity index (F_{31})

(f) Fault endpoint and intersection density (F_{32})

(g) Height of the mine-damaged zone (F_{41})

Fig. 4 Contour maps of the seven assessment factors. **a** Water abundance of the Ordovician limestone aquifer (F_{11}). **b** Water pressure of the Ordovician limestone aquifer (F_{12}). **c** Aquifuge thickness (F_{21}). **d** Brittle rock percentage within the aquifuge (F_{22}). **e** Fault intensity index (F_{31}). **f** Fault endpoint and intersection density (F_{32}). **g** Height of the mine-damaged zone (F_{41})

to express their knowledge precisely. Therefore, the AHP method is often criticized for its inability to adequately deal with the inherent uncertainty and imprecision in the pairwise comparison process (Deng 1999).

To address the vagueness of human thought and uncertainty in real-world decision-making, fuzzy set theory was first introduced by Zadeh (1965); fuzzy set theory, which allows mathematical operators and programming to apply to the fuzzy domain, was first applied to a decision-making problem by Bellman and Zadeh (1970). A fuzzy set is a class of objects with a continuum of grades of membership, which is characterized by a membership function, devoting values between 0 and 1 to the objects (Zadeh 1965). In applications, a fuzzy number is either a TFN or trapezoidal fuzzy number. A TFN, $\widetilde{M}$, is expressed simply as $\widetilde{M}$ (s, m, l) or $\widetilde{M}$ ($s|m$, $m|l$), where s, l, and m are the minimum and maximum possible values and the most promising value, respectively. A fuzzy event can be described by the TFN (Ataei et al. 2012). The left and right sides of each TFN are linear representations, and the membership function of the TFN $\widetilde{M}$ (s, m, l) is expressed as Eq. (3) (Deng 1999):

$$\mu\left(x|\widetilde{M}\right) = \begin{cases} 0, & x < s, \\ (x-s)/(m-s), & s \leq x \leq m \\ (l-x)/(l-m), & m \leq x \leq l \\ 0, & x > l, \end{cases} \quad (3)$$

Compared with a trapezoidal fuzzy number, a TFN is more convenient for computational simplicity, and it is useful in information processing in the fuzzy environment (Ertugrul and Karakasoglu 2009). In this paper, to address the fuzziness of decision makers' judgments in the conventional AHP method, the TFN method was adopted in addition to the AHP method to calculate the weights of the assessment factors. The expert only gives the maximum scores for each factor in the AHP-TFN method, and then the factor comparison matrix is prepared.

The four steps to calculate the weights of the assessment factors with the AHP-TFN method are as follows: (a) establishing the hierarchical structure model; (b) determining the relative importance of the factors in each hierarchy; (c) calculating the weights of the factors in each hierarchy with the TFN method; and (d) determining the total weights of the assessment factors.

Establishing the hierarchical structure model

In this subsection, a structure of the hierarchy with an index layer, criterion layer, and target layer was set up based on the selected assessment factors, as shown in Fig. 5. The target layer of the hierarchy is the water inrush risk of the No. 11 coal seam from the Ordovician aquifer in this study. The criterion layer of the hierarchy, which is the intermediate link for solving the target problem, is formed by four aspects affecting mine water inrush: aquifer (F_1), aquifuge (F_2), geological structure (F_3), and mining (F_4). The index layer, which is the lowest layer in the hierarchal structure model, is constituted by seven quantitative assessment factors: water abundance (F_{11}) and water pressure (F_{12}) of the Ordovician limestone aquifer, aquifuge thickness (F_{21}), brittle rock percentage within the aquifuge (F_{22}), fault intensity index (F_{31}), fault endpoint and intersection density (F_{32}), and height of the mine-damaged zone (F_{41}).

Determination of the relative importance of the factors in each hierarchy

To compute the weights of the assessment factors, it is essential to determine the relative importance of the factors with the Delphi method. The scores of the factors were collected from the experts according to the Saaty rating scale (the 1–9 scale method as shown in Table 1) (Saaty 1980). Based on the hierarchical structure model (Fig. 4), the relative importance of each factor was evaluated in each layer by the invited experts; these results were scored for each layer of the

Fig. 5 Hierarchical structure model
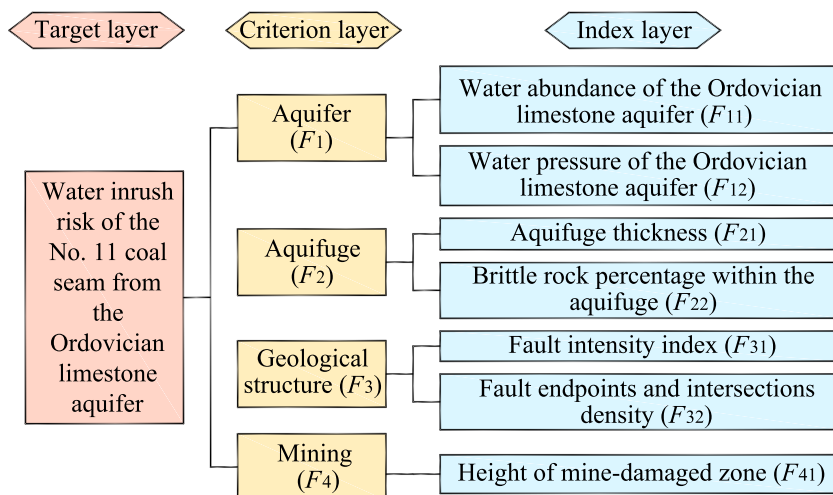
Table 1 The Saaty rating scale (Saaty 1980)

Importance	Definition	Explanation
1	Equally important	Two factors contribute equally to the objective
3	Slightly more important	Experience and judgment slightly favor one factor over another
5	Strongly more important	Experience and judgment strongly favor one factor over another
7	Demonstrably more important	One factor is very strongly favored and its importance is demonstrated in practice
9	Absolutely more important	The evidence favoring one factor over another is of the highest possible validity
2, 4, 6, 8	Intermediate values	When compromise is needed

hierarchical structure model from top to bottom, as shown in Tables 2, 3, 4, 5, and 6.

Calculating the weights of factors in each hierarchy with the TFN method

The TFN method is useful for solving the ambiguity and uncertainty, which was utilized to deal with the fuzziness of the experts' judgments about the relative importance of each factor. The four steps to calculate the weights of the factors in each hierarchy with the TFN method are as follows.

Step 1. Establishing the comparison matrices.

According to the relative importance of the factors in each hierarchy listed in Tables 2, 3, 4, 5, and 6, a pairwise comparison matrix A in each hierarchy is calculated with Eq. (4) (Norouzi and Namin 2019):

$$A = [a_{ij}] = \begin{bmatrix} 1 & a_{12} & \cdots & a_{1n} \\ 1/a_{12} & 1 & \cdots & a_{2n} \\ \vdots & \vdots & \ddots & \vdots \\ 1/a_{1n} & 1/a_{2n} & \cdots & 1 \end{bmatrix} \quad (4)$$

where a_{ij} indicates a quantified judgment of the relative importance of the factors F_i and F_j, where $i, j = 1, 2, \ldots, n$; n is the total number of factors in each hierarchy; F_i and F_j represent the ith and jth factors, respectively; and $a_{ji} = 1/a_{ij}$.

Step 2. Computing the fuzzy pairwise comparison matrix.

For this study, the TFN $\tilde{a}_{ij}$ was defined by Eq. (5) (Hayaty et al. 2014):

$$\tilde{a}_{ij} = \left(\alpha_{ij}, \beta_{ij}, \gamma_{ij} \right) = \left(\text{Min}(a_{ijk}), \left(\prod_{k=1}^{m} a_{ijk} \right), \text{Max}(a_{ijk}) \right) \quad (5)$$

where α_{ij}, β_{ij}, and γ_{ij} indicate the lower bound, geometric mean, and upper bound; a_{ijk} is the quantified judgment of the relative importance on the factors F_i and F_j given by the kth expert; $i, j = 1, 2, \ldots, n$, and n is the total number of factors in each hierarchy; $k = 1, 2, \ldots, m$, and m is the total number of experts.

This provided the fuzzy pairwise comparison matrix $\tilde{A}$ (Hayaty et al. 2014), shown as Eq. (6):

$$\tilde{A} = [\tilde{a}_{ij}] = \begin{bmatrix} (1, 1, 1) & (\alpha_{12}, \beta_{12}, \gamma_{12}) & \cdots & (\alpha_{1n}, \beta_{1n}, \gamma_{1n}) \\ (1/\gamma_{12}, 1/\beta_{12}, 1/\alpha_{12}) & (1, 1, 1) & \cdots & (\alpha_{2n}, \beta_{2n}, \gamma_{2n}) \\ \vdots & \vdots & \ddots & \vdots \\ (1/\gamma_{1n}, 1/\beta_{1n}, 1/\alpha_{1n}) & (1/\gamma_{2n}, 1/\beta_{2n}, 1/\alpha_{2n}) & \cdots & (1, 1, 1) \end{bmatrix} \quad (6)$$

Step 3. Calculating the fuzzy synthetic extent of the ith factor ($\tilde{S}_i$), which is expressed as Eq. (7) (Chatterjee et al. 2015; Rezaei et al. 2015):

Table 2 Relative importance of the factors in the criterion layer

	1st expert (E_1)	2nd expert (E_2)	3rd expert (E_3)
F_1	7	6	5
F_2	6	6	5
F_3	7	6	6
F_4	6	4	5

Table 3 Relative importance of the factors $F_1 \sim F_{1t}$ ($t = 1$–2)

F_1	E_1	E_2	E_3
F_{11}	5	6	6
F_{12}	4	7	7

Table 4 Relative importance of the factors $F_2 \sim F_{2t}$ ($t = 1$–2)

F_2	E_1	E_2	E_3
F_{21}	8	7	6
F_{22}	5	7	5

$$\widetilde{S}_i = \widetilde{r}_i \otimes \left(\widetilde{r}_1 \oplus \widetilde{r}_2 \oplus \cdots \oplus \widetilde{r}_n \right)^{-1} \tag{7}$$

where $\widetilde{r}_i = (a_{i1} \otimes a_{i2} \otimes ... \otimes a_{in})^{1/n}$; $i = 1, 2, …, n$, and n is the total number of factors in each hierarchy; and the symbols $\otimes$ and $\oplus$ denote the multiplication and additive operation of fuzzy numbers, respectively.

Step 4. Determining the weights of the factors in each hierarchy.

Assuming two triangular fuzzy numbers $\widetilde{S}_1 = (\alpha_1, \beta_1, \gamma_1)$ and $\widetilde{S}_2 = (\alpha_2, \beta_2, \gamma_2)$, the possibility degree of $\widetilde{S}_2 \geq \widetilde{S}_1$ is expressed by Eq. (8) (Chang 1996):

$$P\left(\widetilde{S}_2 \geq \widetilde{S}_1\right) = \mu_{S_2}(d)$$
$$= \begin{cases} 1 & \text{if } \beta_2 \geq \beta_1 \\ \dfrac{\alpha_1 - \gamma_2}{(\beta_2 - \gamma_2) - (\beta_1 - \alpha_1)} & \text{if } \beta_2 < \beta_1, \gamma_2 \geq \alpha_1 \\ 0 & \text{otherwise} \end{cases} \tag{8}$$

where $P\left(\widetilde{S}_2 \geq \widetilde{S}_1\right)$ is the possibility degree of $\widetilde{S}_2 \geq \widetilde{S}_1$; d denotes the highest ordinate of the crossing point between $\mu_{\widetilde{S}_1}$ and $\mu_{\widetilde{S}_2}$ to compare $\widetilde{S}_2$ and $\widetilde{S}_1$; and $\mu_{\widetilde{S}_1}$ and $\mu_{\widetilde{S}_2}$ are the membership functions of $\widetilde{S}_2$ and $\widetilde{S}_1$, respectively. The possibility degree of a convex fuzzy number $\widetilde{S}$ that is larger than $\widetilde{S}_i$ ($i = 1, 2, …, n$) can be expressed as Eq. (9) (Ataei et al. 2012):

$$P\left(\widetilde{S} \geq \widetilde{S}_1, \widetilde{S}_2, \cdots, \widetilde{S}_n\right) = P\left[\left(\widetilde{S} \geq \widetilde{S}_1\right), \left(\widetilde{S} \geq \widetilde{S}_2\right), \cdots, \left(\widetilde{S} \geq \widetilde{S}_n\right)\right]$$
$$= \min P\left(\widetilde{S} \geq \widetilde{S}_i\right), i = 1, 2, …, n \tag{9}$$

Assuming $d(F_j) = \min P\left(\widetilde{S}_j \geq \widetilde{S}_i\right)$ where $i = 1, 2, …, n$; $j \neq i$, the weight vector of factors in each hierarchy is expressed by Eq. (10) (Ataei et al. 2012):

$$w' = (d(F_1), d(F_2), \cdots, d(F_n))^{\mathrm{T}} \tag{10}$$

where w' is the weight vector of the factors in each hierarchy and F_j is the jth factor, where $j = 1, 2, …, n$ and n is the total number of factors in each hierarchy.

Finally, the normalized weight vector of the factors in each hierarchy is determined by Eq. (11) (Yin et al. 2018):

$$w = \left(\frac{d(F_1)}{\sum_{i=1}^n d(F_i)}, \frac{d(F_2)}{\sum_{i=1}^n d(F_i)}, \cdots, \frac{d(F_n)}{\sum_{i=1}^n d(F_i)} \right)^{\mathrm{T}} \tag{11}$$

For example, to calculate the weights of the factors in the criterion layer, four factors, F_1, F_2, F_3, and F_4, and three experts were used. Three 4×4 pairwise comparison matrices based on the data in Table 2 were established via Eq. (4) as follows:

$$A_1 = \begin{bmatrix} 1.000 & 1.167 & 1.000 & 1.167 \\ 0.857 & 1.000 & 0.857 & 1.000 \\ 1.000 & 1.167 & 1.000 & 1.167 \\ 0.857 & 1.000 & 0.857 & 1.000 \end{bmatrix}, \quad A_2 = \begin{bmatrix} 1.000 & 1.000 & 1.000 & 1.500 \\ 1.000 & 1.000 & 1.000 & 1.500 \\ 1.000 & 1.000 & 1.000 & 1.500 \\ 0.667 & 0.667 & 0.667 & 1.000 \end{bmatrix}, \quad A_3 = \begin{bmatrix} 1.000 & 1.000 & 0.833 & 1.000 \\ 1.000 & 1.000 & 0.833 & 1.000 \\ 1.200 & 1.200 & 1.000 & 1.200 \\ 1.000 & 1.000 & 0.833 & 1.000 \end{bmatrix}$$

Applying Eqs. (5) and (6), we can obtain the fuzzy pairwise comparison matrix $\widetilde{A}$ as follows:

$$\widetilde{A} = \begin{bmatrix} (1.000, 1.000, 1.000) & (1.000, 1.053, 1.167) & (0.833, 0.941, 1.000) & (1.000, 1.205, 1.500) \\ (0.857, 0.950, 1.000) & (1.000, 1.000, 1.000) & (0.833, 0.894, 1.000) & (1.000, 1.145, 1.500) \\ (1.000, 1.063, 1.200) & (1.000, 1.119, 1.200) & (1.000, 1.000, 1.000) & (1.167, 1.281, 1.500) \\ (0.667, 0.830, 1.000) & (0.667, 0.874, 1.000) & (0.667, 0.781, 0.857) & (1.000, 1.000, 1.000) \end{bmatrix}$$

The fuzzy synthetic extent values of factors F_1, F_2, F_3, and F_4 were calculated with Eq. (7) as follows (Table 6):

Table 5 Relative importance of the factors $F_3 \sim F_{3t}$ ($t = 1$–2)

F_3	E_1	E_2	E_3
F_{31}	7	7	8
F_{32}	5	7	6

$$\widetilde{S}_1 = (0.833, 1.194, 1.750) \otimes (3.011, 4.254, 6.267)^{-1}$$
$$= (0.133, 0.281, 0.581)$$

Table 6 Relative importance of the factors $F_4 \sim F_{41}$

F_4	E_1	E_2	E_3
F_{41}	5	5	5

$\widetilde{S}_2 = (0.714, 0.972, 1.500) \otimes (3.011, 4.254, 6.267)^{-1}$

$\quad = (0.114, 0.228, 0.498)$

$\widetilde{S}_3 = (1.167, 1.522, 2.160) \otimes (3.011, 4.254, 6.267)^{-1}$

$\quad = (0.186, 0.358, 0.717)$

$\widetilde{S}_4 = (0.296, 0.566, 0.857) \otimes (3.011, 4.254, 6.267)^{-1}$

$\quad = (0.047, 0.133, 0.285)$

In the next step, the calculated fuzzy synthetic extent values were compared with Eq. (8) as follows:

$P\left(\widetilde{S}_1 \geq \widetilde{S}_2\right) = 1.000, P\left(\widetilde{S}_1 \geq \widetilde{S}_3\right) = 0.837, P\left(\widetilde{S}_1 \geq \widetilde{S}_4\right) = 1.000,$
$P\left(\widetilde{S}_2 \geq \widetilde{S}_1\right) = 0.873, P\left(\widetilde{S}_2 \geq \widetilde{S}_3\right) = 0.706, P\left(\widetilde{S}_2 \geq \widetilde{S}_4\right) = 1.000,$
$P\left(\widetilde{S}_3 \geq \widetilde{S}_1\right) = 1.000, P\left(\widetilde{S}_3 \geq \widetilde{S}_2\right) = 1.000, P\left(\widetilde{S}_3 \geq \widetilde{S}_4\right) = 1.000,$
$P\left(\widetilde{S}_4 \geq \widetilde{S}_1\right) = 0.507, P\left(\widetilde{S}_4 \geq \widetilde{S}_2\right) = 0.643, P\left(\widetilde{S}_4 \geq \widetilde{S}_3\right) = 0.306,$

After that, priority weights were calculated with Eq. (9) as follows:

$d(F_1) = \min(1.000, 0.837, 1.000) = 0.837,$

$d(F_2) = \min(0.873, 0.706, 1.000) = 0.706,$

$d(F_3) = \min(1.000, 1.000, 1.000) = 1.000,$

$d(F_4) = \min(0.507, 0.643, 0.306) = 0.306.$

By these evaluations, the weight vector in the criterion layer was obtained as by Eq. (10) as $w' = (0.837, 0.707, 1.000, 0.305)^T$. Finally, the normalized weight vector of factors in the criterion layer was determined by Eq. (11) as follows (Table 6):

$w = (0.294, 0.248, 0.351, 0.107)^T$

Similarly, here, the normalized weights of factors in the hierarchy $F_1 \sim F_{1t}$ (t = 1–2), $F_2 \sim F_{2t}$ (t = 1–2), $F_3 \sim F_{3t}$ (t = 1–2), and $F_4 \sim F_{41}$ were determined by using Eqs. (3)–(11), as shown in Table 6.

Determining the total weights of the assessment factors

After determining the normalized weight vector of factors in each hierarchy (Table 6), the total weights of seven assessment factors were calculated with Eq. (12) (Li and Chen 2016):

$$W_{st} = w_s \cdot w_{st} \tag{12}$$

where W_{st} is the total weight of the tth assessment factor in the index layer belonging to the sth factor in the criterion layer in Fig. 5; w_s is the normalized weight of the sth factor in the criterion layer; and w_{st} is the normalized weight of the tth assessment factor in the index layer belonging to the sth factor in the criterion layer.

Finally, each assessment factor's total weight was calculated based on the data in Table 7 by using Eq. (12), as shown in Table 7.

Building the water inrush risk index

A multifactor comprehensive evaluation method is considered to be effective when it accounts for all the factors controlling water inrush. In this paper, the TOPSIS method, which is a multifactor comprehensive evaluation method applied to a wide variety of decision problems (Baykasoğlu and Gölcük 2017; Norouzi and Namin 2019; Sepehr and Zucca 2012), was employed to rank the risk of water inrush of the No. 11 coal seam from the Ordovician aquifer by using available geological exploration data. The three steps used to build the WIRI model by the TOPSIS method are as follows:

Step 1. Constructing the weighted standardized matrix.

Based on the data of the seven selected factors in all the samples, the initial decision matrix was first constructed with Eq. (13) (Baykasoğlu and Gölcük 2017; Mikaeil et al. 2011):

$$B = \begin{bmatrix} b_{11} & b_{12} & \cdots & b_{1n} \\ b_{21} & b_{22} & \cdots & b_{2n} \\ \vdots & \vdots & \ddots & \vdots \\ b_{l1} & b_{l2} & \cdots & b_{ln} \end{bmatrix} \tag{13}$$

Table 7 Fuzzy and normalized weights of the factors in each layer, and total weights of the assessment factors

Target layer	Criterion layer	Fuzzy weights	Normalized weights	Index layer	Fuzzy weights	Normalized weights	Total weights
Water inrush risk of the No. 11 coal seam from the Ordovician limestone aquifer	F_1	(0.133, 0.281, 0.581)	0.294	F_{11}	(0.355, 0.486, 0.754)	0.484	0.142
				F_{12}	(0.331, 0.514, 0.704)	0.516	0.152
	F_2	(0.114, 0.228, 0.498)	0.248	F_{21}	(0.385, 0.607, 0.985)	0.658	0.163
				F_{22}	(0.240, 0.393, 0.615)	0.342	0.085
	F_3	(0.186, 0.358, 0.717)	0.351	F_{31}	(0.417, 0.603, 0.817)	0.690	0.242
				F_{32}	(0.298, 0.397, 0.583)	0.310	0.109
	F_4	(0.047, 0.133, 0.285)	0.107	F_{41}	(1.000, 1.000, 1.000)	1.000	0.107

where B is the initial decision matrix; l and n indicate the number of samples to be assessed and the number of factors concerned; b_{pi} indicates the observed value of the ith factor of the pth sample; $p \in [1, l]$; and $i \in [1, n]$.

According to the total weights of the assessment factors in Table 7 and the initial decision matrix, the weighted standardized matrix was then established by normalization and weighting with Eq. (14) (Sepehr and Zucca 2012):

$$V = \left(v_{pi}\right)_{l \times n} = \begin{bmatrix} W_1 c_{11} & W_2 c_{12} & \cdots & W_n c_{1n} \\ W_1 c_{21} & W_2 c_{22} & \cdots & W_n c_{2n} \\ \vdots & \vdots & \ddots & \vdots \\ W_1 c_{l1} & W_2 c_{l2} & \cdots & W_n c_{ln} \end{bmatrix} \quad (14)$$

where V and v_{pi} denote the weighted standardized matrix, and the weighted standardized value of the ith factor of the pth sample; W_i denotes the total weight of the ith factor, $i \in [1, n]$; c_{pi} denotes the standardized value of the ith factor of the pth sample, calculated with Eq. (15) (Sepehr and Zucca 2012):

$$c_{pi} = b_{pi} / \sqrt{\sum_{p=1}^{l} b_{pi}^2}, \quad i = 1, 2, \cdots, n \quad (15)$$

Step 2. Determining the ideal solutions for water inrush.

During the determination of the ideal solutions for water inrush, the potential negative and positive related factors of the water inrush problem must be taken into account separately. The higher the value of the potential negative related factor, the less likely that water inrush would happen, while a higher value of the positive related factor indicated a higher likelihood of water inrush. Therefore, the negative ideal solution (NIS) for water inrush is the maximum value for the negative factors and the minimum value for the positive factors, while the positive ideal solution (PIS) for water inrush is the minimum value for the negative factors and the maximum value for the positive factors. If J_1 and J_2 indicate the set of negative factors and positive factors, respectively, the NIS and PIS are determined by Eqs. (16) and (17) (Li et al. 2013):

$$V^- = \left\{ \left(\max_{1 \le p \le l} v_{pi} \middle| i \in J_1 \right), \left(\min_{1 \le p \le l} v_{pi} \middle| i \in J_2 \right) \right\} \quad (16)$$

$$V^+ = \left\{ \left(\min_{1 \le p \le l} v_{pi} \middle| i \in J_1 \right), \left(\max_{1 \le p \le l} v_{pi} \middle| i \in J_2 \right) \right\} \quad (17)$$

where V^- and V^+ denote NIS and PIS, respectively; J_1 and J_2 denote the sets of negative factors and positive factors, respectively; v_{pi} indicates the weighted standardized value of the ith factor of the pth sample; $p \in [1, l]$; $i \in [1, n]$; and l and n indicate the number of samples to be assessed and the number of factors concerned.

Step 3. Determination of the final ranking of the water inrush risk for each sample.

According to the TOPSIS technique, the greatest risk would be for the sample that is farthest from the NIS and nearest to the PIS. The WIRI for each sample was defined with Eq. (18) (Li et al. 2013):

$$\mathrm{WIRI}_p = \frac{D_p^-}{D_p^+ + D_p^-} = \frac{\sqrt{\sum_{i=1}^{n} \left(v_{pi} - v_i^-\right)^2}}{\sqrt{\sum_{i=1}^{n} \left(v_{pi} - v_i^+\right)^2} + \sqrt{\sum_{i=1}^{n} \left(v_{pi} - v_i^-\right)^2}}, (p = 1, 2, \cdots, l) \quad (18)$$

where WIRI $_p$ is the water inrush risk index of the pth sample; D_p^- is the distance of the pth sample to the NIS; D_p^+ indicates the distance of the pth sample to the PIS; v_{pi} is the weighted standardized value of the ith factor of the pth sample; and v_i^- and v_i^+ are the values of the ith factor in the sets V^- and V^+, respectively.

A larger WIRI value indicates a higher likelihood of water inrush. By arranging WIRI in descending order, a ranking of water inrush risk was determined.

Results and discussion

Results and validation of the predictions

A grid was constructed by using 100 m × 100 m grid units in each thematic map of the assessment factors. The data of the seven assessment factors in 1378 grid units and the three water inrush cases that occurred in the adjacent coal mine, which formed 1381 assessment samples, were gathered to construct a 1381 × 7 initial decision matrix. The initial decision matrix was normalized by using Eq. (15), and then the weighted standardized matrix was formed by multiplying each standardized value and their weights determined by the TFN-AHP method shown in Table 7.

Based on the weighted standardized matrix, the PIS and NIS for water inrush were then determined. In this study, five assessment factors, F_{11}, F_{12}, F_{31}, F_{32}, and F_{41}, which belong to set J_2, were determined to have positive correlations with water inrush, and two assessment factors, F_{21} and F_{22}, which belong to set J_1, have negative correlations with floor water inrush. Therefore, the PIS and NIS for water inrush were then determined with Eqs. (16) and (17) as:

$V^- = \{0.0000, 0.0009, 0.0055, 0.0028, 0.0000, 0.0000, 0.0026\}$, and
$V^+ = \{0.0128, 0.0083, 0.0037, 0.0016, 0.0577, 0.0193, 0.0033\}$.

Finally, the WIRI for each sample was calculated based on the distance of each assessment sample to the PIS and NIS in regard to each criterion by using Eq. (18), by which the final ranking of water inrush risk of the No. 11 coal seam from the

Ordovician aquifer was determined for each assessment sample. Then, all the WIRI data were processed with Golden Software Surfer 13.0, and a WIRI contour map was established (Fig. 6). As shown in Fig. 6, the water inrush risk as represented by the WIRI ranges from 0.023 to 0.786 in the Zhaizhen coal mine.

A total of 190 samples of these 1381 samples were gathered to test the prediction results, of which there were 187 samples (in 15 working faces) where safe extraction was achieved and three samples representing the occurrence of water inrushes from the Ordovician aquifer (Fig. 6 and Table 8). The WIRI values of the samples representing water inrush (Nos. T1, T2, T3) were not less than 0.100, and the WIRI values of the samples where safe extraction was achieved were not larger than 0.094 (Table 8). The results show that the risk ranking of samples with water inrush were higher than that of samples where safe extraction was achieved, demonstrating that the predictions by the WIRI method are in accordance with real-world situations. Therefore, the prediction accuracy based on the WIRI method is 100% (Table 8).

After validation, based on the geometric mean method of the WIRI values of samples with water inrush and samples with safe extraction, the water inrush risk of the No.11 coal seam was divided into two zones:

- I: safe area (WIRI < 0.097), where water inrushes are unlikely, mainly situated in the southwestern and eastern parts of the Zhaizhen coal mine;
- II: dangerous area (WIRI ≥ 0.097), with a higher probability of water inrush, includes the northern, northwestern, and a small area of the southern Zhaizhen coal mine, which was further classified into two subzones:

- II-1: moderately dangerous area (0.097 ≤ WIRI < 0.135);
- II-2: extremely dangerous area (WIRI ≥ 0.135).

Discussions

Relationship between water inrush and the selection factors

It is a challenging and difficult task to accurately predict the risk of water inrush. The aspects affecting water inrush were considered to be the aquifer, aquifuge, geological structure, and mining, described via seven factors: water abundance, water pressure of the Ordovician limestone aquifer, aquifuge thickness, brittle rock percentage within the aquifuge, fault intensity index, fault endpoint and intersection density, and the height of the mine-damaged zone.

Based on the TFN and AHP methods, the weights of the four aspects, aquifer, aquifuge, geological structure, and mining, are 0.294, 0.248, 0.351, and 0.107, respectively, and each of the seven factors considered in this study influences water inrush, with weights of 0.142, 0.152, 0.163, 0.085, 0.242, 0.109, and 0.107, respectively (Table 6, Fig. 7). The geological structure, represented by the fault intensity index and fault endpoint and intersection density, is considered critical to water inrush, and the fault intensity index is the most important factor affecting water inrush. The aquifer and aquifuge also have a strong influence on water inrush. The aquifer is positively related to water inrush, including the water abundance and water pressure of the Ordovician limestone aquifer. The aquifuge, resented by two factors, aquifuge thickness and brittle rock percentage within the aquifuge, has a positive relation with water inrush, and the aquifuge thickness has a more important role in the resistance to water inrush. Mining activities

Fig. 6 Zoning map determined via the WIRI method of the water inrush risk of the No. 11 coal seam from the Ordovician aquifer
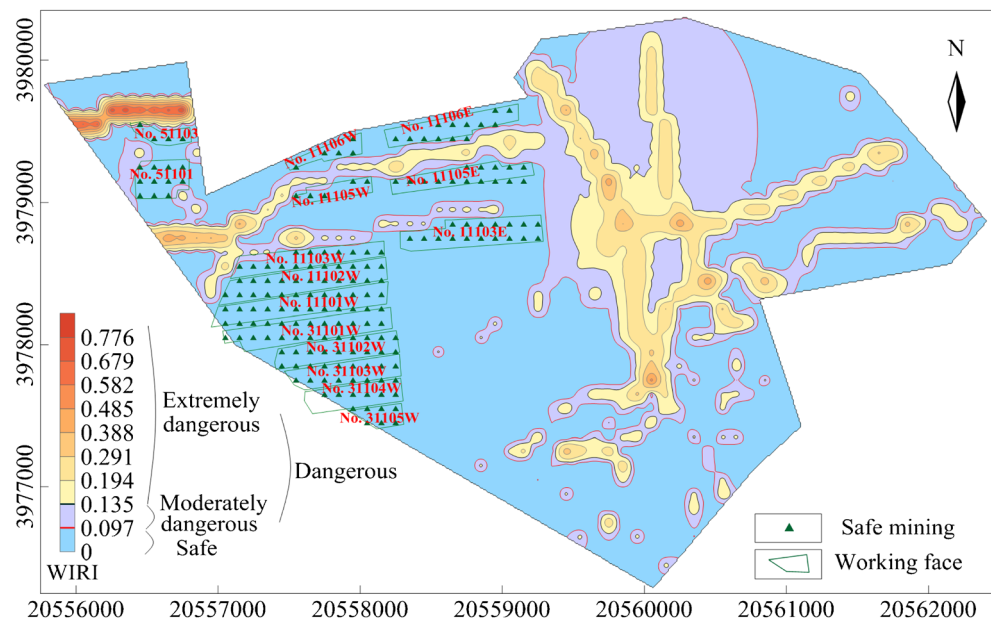
**Table 8** Prediction results by the WIRI method

Working face or water inrush case	Sample no.	WIRI	Actual	Predicted by WIRI method
No. 51103	38, 51, 63, 76	0.081–0.086	Safe	Safe
No. 51101	41, 42, 43, 53, 54, 55, 65, 66, 67, 78, 79	0.080–0.094	Safe	Safe
No. 11102W	119, 130, 131, 142, 143, 156, 157, 170, 171, 185, 202, 219, 220, 238, 239, 258, 259, 279, 280, 300, 301	0.028–0.063	Safe	Safe
No. 11101W	120,121, 132, 133, 144, 145, 158, 172, 186, 187, 203, 204, 221, 222, 240, 241, 260, 261, 281, 302	0.030–0.061	Safe	Safe
No. 31101W	122, 134, 146, 159, 160, 173, 174, 188, 189, 205, 206, 223, 224, 242, 243, 262, 282, 283, 303, 304	0.033–0.061	Safe	Safe
No. 11103W	129, 141, 155, 169, 183, 184, 200, 201, 218, 237, 257, 278, 299	0.035–0.062	Safe	Safe
No. 31102W	175, 176, 190, 191, 207, 208, 225, 244, 263, 264, 284, 285, 305, 306, 327, 328	0.036–0.053	Safe	Safe
No. 11106W	177, 211, 230, 249, 250	0.060–0.064	Safe	Safe
No. 11105W	179, 196, 214, 252, 273	0.061–0.068	Safe	Safe
No. 31103W	192, 209, 226, 227, 245, 246, 265, 266, 286, 287, 307, 308, 329	0.039–0.050	Safe	Safe
No. 31104W	228, 247, 267, 268, 288, 309, 330, 331	0.039–0.048	Safe	Safe
No. 31105W	289, 290, 310, 311, 332, 333	0.042–0.050	Safe	Safe
No. 11106E	313, 337, 361, 385, 386, 411, 412, 438, 439, 465, 492, 493, 520	0.066–0.082	Safe	Safe
No. 11105E	316, 340, 364, 389, 415, 441, 442, 468, 469, 496, 497, 524, 525, 555, 556	0.057–0.082	Safe	Safe
No. 11103E	344, 368, 393, 418, 419, 445, 446, 472, 473, 500, 501, 528, 529, 559, 560, 592, 593	0.040–0.085	Safe	Safe
Water inrush case	T1	0.176	Water inrush	Water inrush
Water inrush case	T2	0.100	Water inrush	Water inrush
Water inrush case	T3	0.103	Water inrush	Water inrush

are taken into account for the assessment of the water inrush risk via one factor: the height of the mine-damaged zone has a weight of 0.107, indicating that this factor also affects the occurrence of water inrush.

Comparison of the predictions by the WIRI method, *T* method, and AHP method

Comparison of the predictions by the WIRI and T methods

The *T* method was proposed in 1964 and has since been
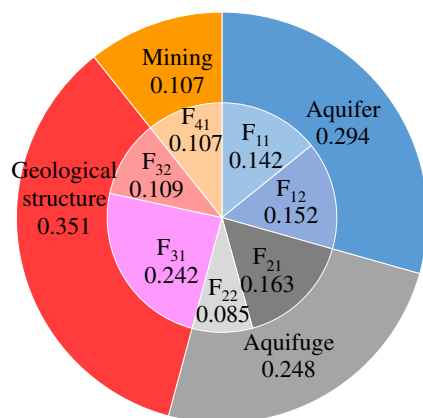
**Fig. 7** Pie diagram of weights of factors

widely used in China, and was calculated with Eq. (19) according to the *Coal Mine Water Control Rules* (Ministry of Coal Industry 2018):

$$T = \frac{F_{12}}{F_{21}} \tag{19}$$

where *T* indicates the water inrush coefficient (MPa/m) and F_{12} and F_{21} indicate the aquifer water pressure (MPa) and aquifuge thickness (m), respectively. The water inrush risk is determined by the *T* method: water inrush is prone to occur when *T* is larger than 0.06 MPa/m in the areas with simple structures or when *T* is larger than 0.10 MPa/m in areas with complex structures; otherwise, water inrush tends not to occur. Figure 8 shows the zoning map of the water inrush risk of the No. 11 coal seam from the Ordovician aquifer by *T*, which was processed and mapped with Golden Software Surfer 13.0.

Based on the results of the 190 test samples (187 safe mining samples and three water inrush samples from the Ordovician aquifer), the predictions by the *T* method do not agree well with the observations: the 187 safe mining samples were all classified as safe, while the three water inrush samples were also classified as safe (Table 9). Based on the 190 test samples, the prediction accuracy of the *T* method is 98.4%,

Fig. 8 Zoning map of the water inrush risk of the No. 11 coal seam from the Ordovician aquifer by the *T* method
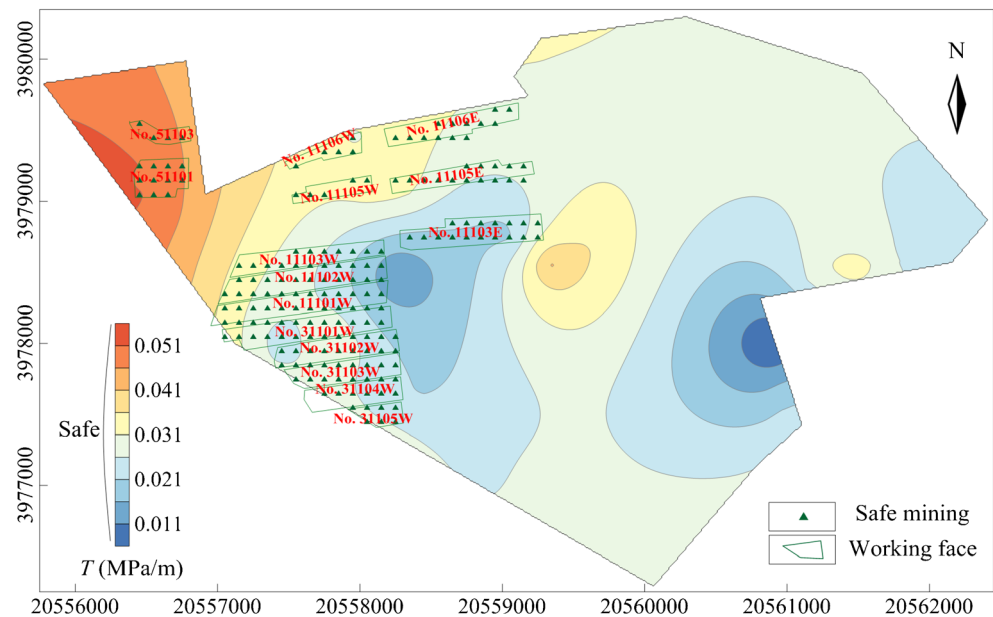
but the samples representing water inrush are not recognized, which will lead to serious consequences. Thus, the results show that the WIRI method proposed in this study has a higher accuracy than that of the *T* method.

Comparison of the predictions by the WIRI and AHP methods

The AHP method, another important method, integrates multiple factors and plays an important role in assessing the probability of water inrush. The details and steps of AHP were described by Malczewski (1999) and Adiat (2012). Accordingly, the weights of the factors in each hierarchy were calculated based on the data in Tables 2, 3, 4, 5, and 6, and the total weights of seven assessment factors were calculated with Eq. (12). Then, the vulnerability index of floor water inrush was established as follows (Wu et al. 2011):

$$
\begin{aligned}
\mathrm{VI} = \sum_{i=1}^{n} W_i f_i(x,y) = {}& 0.110 f_1(x,y) \\
& + 0.130 f_2(x,y) \\
& + 0.140 f_3(x,y) \\
& + 0.114 f_4(x,y) \\
& + 0.156 f_5(x,y) \\
& + 0.140 f_6(x,y) \\
& + 0.211 f_7(x,y) \quad (20)
\end{aligned}
$$

where VI is the vulnerability index, W_i is the weight of the assessment factors, and $f_i(x,y)$ is the contribution function of the normalized value. x and y are the geographical coordinates, and n is the number of assessment factors.

Finally, the VI for each sample was calculated based on Eq. (20); and all the VI data were processed with Golden Software

Surfer 13.0, and a VI contour map was established (Fig. 9). As shown in Fig. 9, the water inrush risk as represented by VI ranges from 0.013 to 0.068 in the Zhaizhen coal mine.

Based on the 190 test samples, the predictions by the AHP method do not agree well with the observations. The VI values of the water inrush samples (Nos. T1, T2, T3) were 0.033, 0.019, and 0.022. There were 19 safely extracted samples whose VI values were larger than 0.019, which was larger than the VI value of a sample with water inrush, T2 (Table 9). That is, these 19 safe mining samples were classified as water inrush. Based on the 190 test samples, the prediction accuracy of the AHP method is 90%. The results show that the WIRI method proposed in this study has a higher accuracy than that of the AHP method.

The zones of water inrush risk predicted by the WIRI and *T* methods were compared (Figs. 6 and 8), indicating that there is a larger difference between these two evaluations. For 62% of all assessment samples, the predictions by these two methods are the same, which were all classified as safe by these two methods and were mainly situated in the southwestern and eastern areas (in Figs. 6 and 8), which are characterized by a low fault intensity and fault endpoint and intersection density, poor water abundance, high brittle rock percentage, and small height of the mine-damaged zone. For 38% of all assessment samples, the predictions by these two methods are contradictory: these samples were determined to be dangerous by the WIRI method, but were determined to be safe by the *T* method, mainly in small areas of the southern, northern, and northwestern parts of the study area (Figs. 6 and 8), which is characterized by a low percentage of brittle rock, complex geological structure, rich water abundance, high water pressure and large height of the mine-damaged zone (Fig. 4). This difference in the predictions is mainly because only

Table 9　Prediction results by the *T* and AHP methods

| Working face or water inrush case	Sample no.	*T*	VI	Actual	Prediction results	
					T method	AHP method
No. 51103	38, 51, 63, 76	0.046–0.049	0.018–0.019	Safe	Safe	Safe-water inrush
No. 51101	41, 42, 43, 53, 54, 55, 65, 66, 67, 78, 79	0.046–0.051	0.018–0.020	Safe	Safe	Safe-water inrush
No. 11102W	119, 130, 131, 142, 143, 156, 157, 170, 171, 185, 202, 219, 220, 238, 239, 258, 259, 279, 280, 300, 301	0.015–0.035	0.015–0.017	Safe	Safe	Safe
No. 11101W	120,121, 132, 133, 144, 145, 158, 172, 186, 187, 203, 204, 221, 222, 240, 241, 260, 261, 281, 302	0.016–0.035	0.015–0.017	Safe	Safe	Safe
No. 31101W	122, 134, 146, 159, 160, 173, 174, 188, 189, 205, 206, 223, 224, 242, 243, 262, 282, 283, 303, 304	0.018–0.034	0.015–0.017	Safe	Safe	Safe
No. 11103W	129, 141, 155, 169, 183, 184, 200, 201, 218, 237, 257, 278, 299	0.018–0.035	0.015–0.017	Safe	Safe	Safe
No. 31102W	175, 176, 190, 191, 207, 208, 225, 244, 263, 264, 284, 285, 305, 306, 327, 328	0.020–0.030	0.015–0.016	Safe	Safe	Safe
No. 11106W	177, 211, 230, 249, 250	0.031–0.034	0.017	Safe	Safe	Safe
No. 11105W	179, 196, 214, 252, 273	0.032–0.034	0.017–0.018	Safe	Safe	Safe
No. 31103W	192, 209, 226, 227, 245, 246, 265, 266, 286, 287, 307, 308, 329	0.022–0.028	0.015–0.016	Safe	Safe	Safe
No. 31104W	228, 247, 267, 268, 288, 309, 330, 331	0.022–0.028	0.015–0.016	Safe	Safe	Safe
No. 31105W	289, 290, 310, 311, 332, 333	0.024–0.027	0.015–0.016	Safe	Safe	Safe
No. 11106E	313, 337, 361, 385, 386, 411, 412, 438, 439, 465, 492, 493, 520	0.029–0.033	0.018–0.020	Safe	Safe	Safe-water inrush
No. 11105E	316, 340, 364, 389, 415, 441, 442, 468, 469, 496, 497, 524, 525, 555, 556	0.026–0.033	0.017–0.020	Safe	Safe	Safe-water inrush
No. 11103E	344, 368, 393, 418, 419, 445, 446, 472, 473, 500, 501, 528, 529, 559, 560, 592, 593	0.020–0.030	0.016–0.019	Safe	Safe	Safe-water inrush
Water inrush case	T1	0.059	0.033	Water inrush	Safe	Water inrush
Water inrush case	T2	0.058	0.019	Water inrush	Safe	Water inrush
Water inrush case	T3	0.040	0.022	Water inrush	Safe	Water inrush

two factors, the water pressure of the Ordovician aquifer and aquifuge thickness, were considered by the *T* method.

And the zones of water inrush risk predicted by the WIRI and AHP methods were compared (Figs. 6 and 9). For 84% of all assessment samples, the predictions by these two methods are the same. While for 16% of all assessment samples, the predictions by these two methods are contradictory: 218 samples were determined to be safe by the WIRI method, but were determined to be dangerous by the AHP method; and two samples were determined to be dangerous by the WIRI method, but were determined to be safe by the AHP method. This difference in the predictions is mainly because AHP method does not consider the vagueness of human thought and uncertainty in real-world decision-making and is a linear model.

In predicted safe areas by the WIRI method, the predictions show a lower risk of water inrush; however, this does not mean that mining these areas is not dangerous. Reporting abnormal observations, such as changes in aquifer water production, variations in water level, and previously concealed faults around the working face, in a timely manner is necessary. Partial dewatering should be performed where abnormalities are found. The dangerous areas are divided into two subzones, moderately and extremely dangerous areas, where the occurrence probabilities of water inrushes are high. The larger the WIRI value, the higher the risk is in the dangerous area. When mining the No.11 coal seam in these areas, the indicators of floor water inrush must be carefully monitored, and preventive measures against water disaster should be taken. Attention should be paid to the changes in the Ordovician limestone water level at all times, and advanced geophysical exploration and drilling should be conducted when the excavation roadway approaches areas with complex hydrogeological conditions. It is also recommended that the Ordovician limestone aquifer be depressurized using dewatering wells and that the hydraulic connectivity with water enrichment areas is reduced by grouting when necessary.

Fig. 9 Zoning map of the water inrush risk of the No. 11 coal seam from the Ordovician aquifer by the AHP method
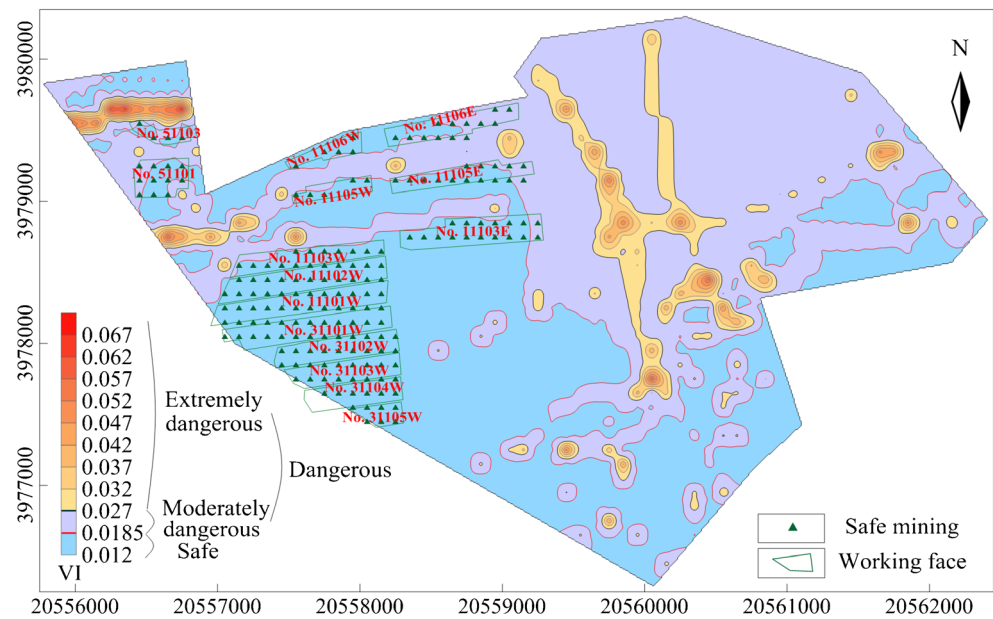
The investigation of geological structures, via methods such as the radio wave penetration method, Rayleigh channel wave prediction method, or other techniques, should be performed to identify small faults in front of any working face (Yang and Cheng 2012). The water content and permeability of the main faults need to be detected by geophysical methods or drilling before mining. Adequate coal pillars need to be retained according to the *Coal Mine Water Control Rules* (Ministry of Coal Industry 2018) for sealing permeable fractures and preventing water inrush from faults.

Conclusions

To prevent coal mine flooding from the underlying Ordovician aquifer in the coal mines of North China coalfields, it is imperative to accurately assess the water inrush risk. A WIRI model based on the TFN-AHP and TOPSIS methods was successfully proposed to assess the water inrush risk of the No. 11 coal seam from the underlying Ordovician aquifer in the Zhaizhen coal mine. Seven main factors were selected for assessing water inrush risk: the water abundance and water pressure of the Ordovician limestone aquifer, aquifuge thickness, brittle rock percentage within the aquifuge, fault intensity index, fault endpoint and intersection density, and height of the mine-damaged zone. The TFN-AHP method was used to determine the factor weights, which were 0.142, 0.152, 0.163, 0.085, 0.242, 0.109, and 0.107 respectively. Each factor plays an important role in water inrush, but the most important factors are the fault intensity index and the aquifuge thickness. A WIRI model was then established using the TOPSIS method based on the weights calculated by the

TFN-AHP method and initial decision data. A zoning map of water inrush risk was built according to the WIRI data with Golden Software Surfer 13.0, and the study area was classified into two zones, the safe area (WIRI < 0.097) and the dangerous area (WIRI ≥ 0.097), which was further classified into two subzones, the moderately dangerous area (0.097 ≤ WIRI < 0.135) and the extremely dangerous area (WIRI ≥ 0.135). This zoning map will provide guidance for safer coal mining and water inrush prevention.

A validation was carried out via data analysis of samples from engineering practice, showing that predictions from the WIRI method conform to actual observations, while the predictions from the *T* method and AHP method do not agree well with the observations. Based on the 190 test samples, the prediction accuracy of the WIRI was 100%, while the prediction accuracies of the *T* and AHP methods were 98.4% and 90%, respectively. Based on the comparison of the results of the WIRI and *T* and AHP methods, the WIRI method proposed in this study has a higher accuracy than those of the *T* and AHP methods. For the *T* method, approximately 38% of the predictions were not in agreement, mainly in small areas of the southern, northern, and northwestern parts of the study area, mainly because only two factors, the water pressure of the Ordovician aquifer and aquifuge thickness, were considered by the *T* method. And for the AHP method, approximately 16% of the predictions were not in agreement, mainly because AHP method does not consider the vagueness of human thought and uncertainty in real-world decision-making and is a linear model.

The results of the case study show that the proposed method can effectively predict the water inrush risk and can be applied to other mines threatened by underlying aquifers.

Moreover, the reliability of the predictions would be further improved with the use of additional data.

References

Ataei M, Mikaeil R, Hoseinie SH, Hosseini SM (2012) Fuzzy analytical hierarchy process approach for ranking the sawability of carbonate rock. Int J Rock Mech Min Sci 50:83–93. https://doi.org/10.1016/j.ijrmms.2011.12.002

Baykasoğlu A, Gölcük İ (2017) Development of an interval type-2 fuzzy sets based hierarchical MADM model by combining DEMATEL and TOPSIS. Expert Syst Appl 70:37–51. https://doi.org/10.1016/j.eswa.2016.11.001

Bednarik RG (2019) Rock metamorphosis by kinetic energy. Emerg Sci J 3(5):293–302. https://doi.org/10.28991/esj-2019-01192

Bellman BE, Zadeh LA (1970) Decision-making in a fuzzy environment. Manag Sci 17(4):141–164. https://doi.org/10.1287/mnsc.17.4.B141

Chang DY (1996) Applications of the extent analysis method on fuzzy AHP. Eur J Oper Res 95:649–655. https://doi.org/10.1016/0377-2217(95)00300-2.

Chang CW, Wu CR, Lin CT, Chen HC (2007) An application of AHP and sensitivity analysis for selecting the best slicing machine. Comput Ind Eng 52(2):296–307. https://doi.org/10.1016/j.cie.2006.11.006

Chatterjee S, Singh JB, Roy A (2015) A structure-based software reliability allocation using fuzzy analytic hierarchy process. Int J Syst Sci 46(3):513–525. https://doi.org/10.1080/00207721.2013.791001

Deng H (1999) Multicriteria analysis with fuzzy pair-wise comparison. Int J Approx Reason 21:215–231. https://doi.org/10.1109/FUZZY.1999.793038

Ertugrul I, Karakasoglu N (2009) Performance evaluation of Turkish cement firms with fuzzy analytic hierarchy process and TOPSIS methods. Expert Syst Appl 36(1):702–715. https://doi.org/10.1016/j.eswa.2007.10.014

Hashemi M, Zadeh HM, Arasteh PD, Zarghami M (2019) Economic and environmental impacts of cropping pattern elements using systems dynamics. Civil Eng J 5(5):1020–1032. https://doi.org/10.28991/cej-2019-03091308

Hayaty M, Tavakoli Mohammadi MR, Rezaei A, Shayestehfar MR (2014) Risk assessment and the ranking of metals using FDAHP and TOPSIS. Mine Water Environ 33(2):157–164. https://doi.org/10.1007/s10230-014-0263-y

Hwang CL, Yoon K (1981) Multiple attribute decision making methods and applications. Springer, New York

Li J (2000) The relations of in-situ rock stress and water-resisting ability for floor aquifuge. Coal Geol Explorat 28(4):47–49 (in Chinese)

Li B, Chen Y (2016) Risk assessment of coal floor water inrush from underlying aquifers based on GRA–AHP and its application. Geotech Geol Eng 34(1):143–154. https://doi.org/10.1007/s10706-015-9935-z

Li P, Qian H, Wu J, Chen J (2013) Sensitivity analysis of TOPSIS method in water quality assessment: I. Sensitivity to the parameter weights. Environ Monit Assess 185:2453–2461. https://doi.org/10.1007/s10661-012-2723-9

Mikaeil R, Yousefi R, Ataei M (2011) Sawability ranking of carbonate rock using fuzzy analytical hierarchy process and TOPSIS approaches. Scientia Iranica B 18(5):1106–1115. https://doi.org/10.1016/j.scient.2011.09.009

Ministry of Coal Industry (2018) Coal mine water control rules. Beijing Publ House of Coal, Industry (in Chinese)

National Bureau of Coal Industry of China (2000) Pillar design and mining regulations under buildings, water, rails and major roadways. China Coal Industry Publ House, Beijing (in Chinese)

Norouzi A, Namin HG (2019) A hybrid fuzzy TOPSIS-best worst method for risk prioritization in megaprojects. Civil Eng J 5(6):1257–1272. https://doi.org/10.28991/cej-2019-03091330

Qiu M, Han J, Zhou Y, Shi LQ (2017) Prediction reliability of water inrush through the coal mine floor. Mine Water Environ 36(2):217–225. https://doi.org/10.1007/s10230-017-0431-y

Qu X, Qiu M, Liu J, Niu Z, Wu X (2019) Prediction of maximal water bursting discharge from coal seam floor based on multiple nonlinear regression analysis. Arab J Geosci 12(18):567. https://doi.org/10.1007/s12517-019-4748-7

Rezaei A, Shayestehfar M, Hassani H, Tavakoli Mohammadi MR (2015) Assessment of metals contamination and their grading by SAW method: a case study in Sarcheshmeh copper complex, Kerman, Iran. Environ Earth Sci 74(4):3191–3205. https://doi.org/10.1007/s12665-015-4356-0

Saaty TL (1980) The analytic hierarchy process. McGraw-Hill, NYC

Sepehr A, Zucca C (2012) Ranking desertification indicators using TOPSIS algorithm. Nat Hazards 62:1137–1153. https://doi.org/10.1007/s11069-012-0139-z

Shi L, Gao W, Han J, Tan X (2017) A nonlinear risk evaluation method for water inrush through the seam floor. Mine Water Environ 36(4):597–605. https://doi.org/10.1007/s10230-017-0449-1

Shi L, Qiu M, Wang Y, Qu X, Liu T (2019a) Evaluation of water inrush from underlying aquifers by using a modified water-inrush coefficient model and water-inrush index model: a case study in Feicheng coalfield, China. Hydrogeol J 27:2105–2119. https://doi.org/10.1007/s10040-019-01985-2

Shi L, Wang Y, Qiu M, Liu T, Zhao Y (2019b) Research on the required width of a fault waterproof coal pillar based on underground pressure control theory. Arab J Geosci 12:480. https://doi.org/10.1007/s12517-019-4637-0

Sun W, Wu Q, Liu H, Jiao J (2015) Prediction and assessment of the disturbances of the coal mining in Kailuan to karst groundwater system. Phys Chem Earth 89-90:136–144. https://doi.org/10.1016/j.pce.2015.10.008

Tahriri F, Mousavi M, Haghighi SH, Dawal SZM (2014) The application of fuzzy Delphi and fuzzy inference system in supplier ranking and selection. J Ind Eng Int 10(3):66. https://doi.org/10.1007/s40092-014-0066-6

Tan Y, Zhao TB, Xiao YX (2010) Researches on floor stratum fracturing induced by antiprocedure mining underneath close-distance goaf. J Min Sci 46(3):250–259. https://doi.org/10.1007/s10913-010-0032-7

Wang X, Meng F (2018) Statistical analysis of large accidents in China's coal mines in 2016. Nat Hazards 92(1):311–325. https://doi.org/10.1007/s11069-018-3211-5

Wang Y, Yang W, Li M, Liu X (2012) Risk assessment of floor water inrush in coal mines based on secondary fuzzy comprehensive evaluation. Int J Rock Mech Min Sci 52:50–55. https://doi.org/10.1016/j.ijrmms.2012.03.006

Wu Q, Zhou W (2008) Prediction of groundwater inrush into coal mines from aquifers underlying the coal seams in China: vulnerability index method and its construction. Environ Geol 55(4):245–254. https://doi.org/10.1007/s00254-007-1160-5

Wu Q, Zhang ZL, Ma JF (2007) A new practical methodology of the coal floor water bursting evaluation I: the master controlling index system construction. J China Coal Soc 32(1):42–47 (in Chinese)

Wu Q, Xu H, Pang W (2008) GIS and ANN coupling model: an innovative approach to evaluate vulnerability of karst water inrush in

coalmines of North China. Environ Geol 54:937–943. https://doi.org/10.1007/s00254-007-0887-3

Wu Q, Liu Y, Liu D, Zhou W (2011) Prediction of floor water inrush: the application of GIS-based AHP vulnerable index method to Donghuantuo Coal Mine, China. Rock Mech Rock Eng 44:591–600. https://doi.org/10.1007/s00603-011-0146-5

Wu Q, Liu Y, Zhou W, Li B, Zhao B, Liu S, Sun W, Zeng Y (2015) Evaluation of water inrush vulnerability from aquifers overlying coal seams in the Menkeqing coal mine, China. Mine Water Environ 34:258–269. https://doi.org/10.1007/s10230-014-0313-5

Wu QS, Jiang LS, Wu QL (2017a) Study on the law of mining stress evolution and fault activation under the influence of normal fault. Acta Geodyn Geomater 14(3):357–369. https://doi.org/10.13168/AGG.2017.0018

Wu Q, Zhao D, Wang Y, Shen J, Mu W (2017b) Method for assessing coal-floor water-inrush risk based on the variable-weight model and unascertained measure theory. Hydrogeol J 25:2089–2103. https://doi.org/10.1007/s10040-017-1614-0

Xu F, Long R, Xia Y, Xie S (1991) Quantitative assessment and prediction of geological structures in coal mine. J China Coal Soc 16(4):93–102 (in Chinese)

Yang S, Cheng J (2012) The method of small structure prediction ahead with Rayleigh channel wave in coal roadway and seismic wave field

numerical simulation. Chinese J Geophys Chin Edition 55:655–662 (in Chinese)

Yang B, Sui W, Liu J (2019) Application of GIS-based decision-making model to evaluate safety of underground mining under Neogene aquifers. Int J Oil Gas Coal Technol 22(1):40–63. https://doi.org/10.1504/IJOGCT.2019.102277

Yin S, Zhang J, Liu D (2015) A study of mine water inrushes by measurements of in situ stress and rock failures. Nat Hazards 79:1961–1979. https://doi.org/10.1007/s11069-015-1941-1

Yin H, Shi Y, Niu H, Xie D, Wei J, Lefticariu L, Xu X (2018) A GIS-based model of potential groundwater yield zonation for a sandstone aquifer in the Juye Coalfield, Shangdong, China. J Hydrol 557:434–447. https://doi.org/10.1016/j.jhydrol.2017.12.043

Zadeh LA (1965) Fuzzy sets. Inf Control 8:338–353. https://doi.org/10.1016/S0019-9958(65)90241-X

Zhang S, Guo W, Li Y (2017) Experimental simulation of water-inrush disaster from the floor of mine and its mechanism investigation. Arab J Geosci 10(22):503. https://doi.org/10.1007/s12517-017-3287-3

Zhao D, Wu Q, Cui F, Xu H, Zeng Y, Cao Y, Du Y (2018) Using random forest for the risk assessment of coal-floor water inrush in Panjiayao Coal Mine, northern China. Hydrogeol J 20(7):2327–2340. https://doi.org/10.1007/s10040-018-1767-5